WISC

UNIVERSITY OF WISCONSIN • MADISON, WISCONSIN

PLASMA PHYSICS

MHD COMPUTATION OF FEEDBACK OF RESISTIVE-SHELL INSTABILITIES IN THE REVERSED FIELD PINCH

E.J. ZITA, S.C. PRAGER, Y.L. HO*, and D.D. SCHNACK*

DOE/ER/53212-195

May 1992

NOTICE

Printed in the United States of America
Available from
National Technical Information Service
U.S. Department of Commerce
5285 Port Royal Road
Springfield, VA 22161

NTIS Price codes
Printed copy: A03
Microfiche copy: A01

MHD computation of feedback of resistive-shell instabilities in the Reversed Field Pinch

E.J. ZITA and S.C. PRAGER (University of Wisconsin, Madison, WI 53706)
Y.L. HO and D.D. SCHNACK (Science Applications International Corporation, San Diego, CA 92121)

DOE/ER/53212--195

DE92 014325

ABSTRACT: MHD computation demonstrates that feedback can sustain reversal and reduce loop voltage in resistive-shell reversed field pinch (RFP) plasmas. Edge feedback on ~2R/a tearing modes resonant near axis is found to restore plasma parameters to nearly their levels with a close-fitting conducting shell. When original dynamo modes are stabilized, neighboring tearing modes grow to maintain the RFP dynamo more efficiently. This suggests that experimentally observed limits on RFP pulselengths to the order of the shell time can be overcome by applying feedback to a few helical modes.

1. INTRODUCTION

The Reversed Field Pinch (RFP) has several attractive features as a possible fusion reactor, including weak magnetic field, high beta, high energy density, and relatively small size. However, one disadvantage is the requirement for a close-fitting conducting shell. Both experiment[1,2,3,4] and theory[5] suggest that the stabilizing influence of the shell is necessary. With a conducting shell, MHD fluctuations saturate and the pulse length is limited only by the available volt-seconds. With a resistive shell, fluctuations grow well above their amplitudes with a conducting shell, with an accompanying increase in the toroidal loop voltage. It has been observed in experiment and MHD computation[6,7] that growing resistive shell modes destroy RFP reversal on the order of the shell time for soak-in of a magnetic field. This presents a fundamental problem, since the stabilizing role of any shell with finite conductivity will vanish on the long

time-scale of a steady-state reactor. The presence of a conducting shell also complicates fine control of the equilibrium by application of a vertical magnetic field.

The dominant RFP fluctuations with either a conducting or resistive shell are internally resonant tearing modes, which are responsible for the dynamo sustainment of the RFP[8]. These modes convert poloidal field into mean toroidal field (B_T) and provide edge reversal of B_T by driving current at the plasma edge through an effective fluctuation-induced electric field $\langle v \times B \rangle$ (where v and B are velocity and magnetic field fluctuations and $\langle\ \rangle$ is an average over the poloidal and toroidal directions). In the plasma core, however, the direction of the fluctuation-induced field is opposed to the applied electric field. Therefore growing dynamo modes also suppress plasma current, and thus necessitate a higher toroidal loop voltage to sustain the current. These resistive shell modes are small in number (approximately equal to the aspect ratio, R/a) and global in spatial structure, with poloidal and toroidal mode numbers m=1, $|n| \geq 2R/a$. We use MHD computation to examine the feasibility, from a physics perspective, of a feedback solution to the resistive shell problem.

Restoration of the helical mode amplitudes and loop voltage to the comducting shell levels would constitute a solution. We investigate edge feedback suppression of these modes as a means of restoring mode amplitudes and loop voltage to conducting shell levels, without suppressing the dynamo. In these tests, the conducting shell is replaced by helical coils which hold the radial magnetic field to zero at the plasma boundary, for a few specific helical modes. This boundary condition for targeted helical modes is easily implemented in a nonlinear, resistive, pseudospectral 3D MHD code. (Linear calculations cannot adequately address the problem since nonlinear mode coupling and quasilinear profile modifications are key to RFP dynamics.[9]) There has been a limited

experimental test of feedback of a single mode[10] which agrees well with our numerical tests. In addition, circuits have been examined for related feedback schemes to address engineering feasibility questions.[11,12]

We find that, in the absence of a conducting shell, selected feedback of the dominant tearing modes resonant near axis reduces their fluctuation amplitudes to nearly the levels with a full conducting shell and improves plasma parameters. The spatial structure of feedback-targeted dynamo modes is also altered so that, to first order, they no longer suppress plasma current nor provide dynamo sustainment. The dynamo role is promptly assumed by neighboring modes in k-space. Feedback on as few as one mode can sustain the RFP for many resistive shell times, permit lower-voltage operation, and reduce flux surface tearing (thereby reducing transport and wall interactions), approaching plasma parameters characteristic with a conducting shell.

In the remainder of this paper, we will review the numerical model used in these calculations (section II), describe the feedback schemes (section III), detail feedback results (section IV), and summarize our work (section V).

2. NUMERICAL MODEL

All calculations presented in this paper were generated with a 3D magnetohydrodynamic (MHD) code[13] with nonideal boundary conditions[14,7]. This program (DEBS) solves the normalized, pressureless, resistive, compressible MHD equations:

$$d\vec{A}/dt = -\eta\vec{J} + S\,\vec{v}\times\vec{b}$$

$$\rho d\vec{v}/dt = -S\rho\,\vec{v}\cdot\nabla\vec{v} + \nu\nabla^2\vec{v} + S\,\vec{J}\times\vec{B}$$

$$\vec{B} = \nabla x \vec{A}$$
$$\vec{J} = \nabla x \vec{B}$$

where the magnetic Reynolds number $S = \tau_R/\tau_A$, and the Alfvén time $\tau_A = a/v_A$. Times are normalized to the resistive diffusion time $\tau_R = \mu_0 a^2/\eta$, velocities are normalized to the Alfvén velocity $v_A = B_0/(\mu_0\rho_0)^{1/2}$, and lengths are normalized to the plasma minor radius, a, where the magnetic field B and mass density ρ are measured in units of a characteristic field B_0 and a characteristic density ρ_0, respectively. The viscous damping parameter ν is chosen for numerical stability. The gauge in which $\nabla\Phi=0$ has been chosen, where Φ is the electrostatic potential.

The DEBS code solves an initial value problem in $\vec{B}$, $\vec{v}$, $\vec{J}$, and $\vec{A}$, starting with modified Bessel-function model profiles typically chosen to yield a pinch parameter $\Theta = 1.59$. In all cases, S is 6000, at least an order of magnitude lower than experimental Reynolds numbers; this results in a narrower numerical mode spectrum than observed experimentally. The pressure gradient is set to zero, valid for low-beta plasmas; this limits differentiation of diffusion and dynamo timescales[15], but accurately models evolution of profiles and flux surface reconnections characteristic of dynamo "sawteeth"[16]. Density ρ and resistivity η profiles are not advanced in time, and plasma current and toroidal flux are held constant once steady state is reached. Conducting wall boundary conditions are maintained as the MHD equations are advanced in time until a steady-state RFP equilibrium is reached. Resistive-shell boundary conditions are then imposed on this equilibrium, which is advanced with or without feedback. Resistive-shell RFPs typically evolve away from the initial equilibrium as fluctuations grow, and fail to reach a true steady state in the absence of feedback.

DEBS pseudo-spectrally models a periodic cylinder of length $L=2\pi R$, where

R is the major radius. Equations are finite-differenced radially and Fourier analyzed in the θ and z directions: linear terms are advanced in Fourier space and nonlinear terms in configuration space, using Fast Fourier Transform (FFT) routines.[17] Use of a semi-implicit algorithm eliminates Alfvén wave time-step constraints and allows tracking of phenomena on longer resistive diffusion timescales[15] . It has been shown numerically that m=2 modes dissipate energy cascaded to short wavelengths, thus are important in determining the width in n-space of the magnetic energy spectrum, but that m > 2 contribute little to RFP dynamics[18] . It has also been shown analytically[19] and experimentally[20,21] that the dominant helical modes have m=1, n≈−2R/a, which resonate near the RFP axis. Higher-n modes (eg -n≈4R/a) resonate closer to the plasma edge, are spaced more closely together, and have amplitudes an order of magnitude lower. Since modes couple as (m,n) + (m′,n′) → (m±m′, n±n′), the smallest scale m=2 modes of significance will have -n ≈8(R/a). Therefore, to include all modes important in the present study, m=0, ±1, ±2 and n=0,±1,±2, ...,±(8R/a) are retained after de-aliasing. The radial grid is resolved to 1/127 minor radius.

3. FEEDBACK SCHEME

The feedback boundary conditions are applied numerically to a mode (m,n) targeted for stabilization by specifying that $B_r(m,n)$ vanish at r=a. (A resistive shell is also situated at the plasma radius a.) The pseudospectral nature of the code is exploited to impose boundary conditions on each helical mode independently. In Fourier space, $B_r = (\nabla\times A)_r = i(mA_z/r - kA_\theta)$, assuming quantities vary as $f(r)e^{i(m\theta + kz + \phi)}$ where k=n/R is the axial wavenumber. Choosing $B_r=0$ determines $A_\theta(m,n)$ and $A_z(m,n)$ for the targeted mode at r=a,

consistent with the remaining boundary conditions: that $J_r=0$, $E_\Theta(a)=0$, $E_Z(a)=$ the edge field applied to sustain plasma current $J = (E_{||} - E_F)/\eta$, and $v(a)=0$ for all modes except that $v_r(a)=-E_Z B_\Theta/SB^2$ for the mean[22].

The feedback boundary condition can be realized experimentally by winding helical current-carrying coils on the resistive shell. The numerical scheme is equivalent to a set of helical coils (one sine and one cosine) to feedback on each mode (m,n), wound with the same pitch as the magnetic field line at r_s with which the mode resonates, where $q(r_s)=m/n$. The helical coils are perfectly conducting, drawing whatever current necessary (from an external power source) to keep $B_r(m,n)=0$ for the targeted mode. There is no time delay between "sensing" an edge B_r and nulling it, and the feedback response is perfectly out of phase with the target mode.

4. FEEDBACK RESULTS

4.1 Description

Our numerical experiment comprises a number of nonlinear resistive-shell RFP runs which suppress different subsets of tearing modes with the feedback scheme described above. We seek to characterize the smallest subset of feedback-targeted modes for which plasma parameters approach the conducting-shell case. Effective feedback should minimize mode growth and loop voltage in the absence of a conducting shell, while maintaining the reversed-field configuration.

Changes in profiles of the parallel fluctuation-induced electric field $E_{F||} = -\langle \vec{v} \times \vec{b} \rangle \cdot \vec{B}/|\vec{B}|$ are key in interpreting results of the various feedback cases presented below. Dominant, axially resonant m=1 tearing modes typically have

positive $E_{F||}(m,n)$ in the core, and negative $E_{F||}(m,n)$ at the edge, changing sign near the modal resonant surface[23]. Since edge $\vec{B}$ is primarily poloidal in the RFP, edge $E_{F||}$ is primarily poloidal Negative E_Θ at a radius r drives toroidal flux inside r, sustaining core B_z against diffusion.[8] Insofar as the shell is a flux conserver, negative flux is generated outside r, which can reverse edge B_z and contribute to RFP stability by enhancing shear. "Dynamo modes" are by definition those supplying the bulk of negative E_Θ near the reversal region. In fact, edge $E_{F||}$ of m=1 tearing modes provides the RFP dynamo[24]. Typically, all internal m=1 modes with $2R/a \leq |n| \leq 3R/a$ are candidate dynamo modes.

Effective feedback must not only maintain negative edge E_F of dominant fluctuations, but should also minimize central E_F. Since $B_\theta \sim 0$ near r=0, central E_F and plasma current are primarily toroidal. Positive E_F near axis suppresses plasma current $\eta J_{||} = E_{||} - E_F$ (or, equivalently, requires higher loop voltage, under a constant-current constraint). Therefore, the an efficient dynamo mode has low E_F in the core in addition to negative $E_F(m,n)$ in the outer region.

The most effective feedback schemes target the subset of candidate dynamo modes which provides the greatest contribution to both dynamo and loop voltage V_L. Feedback decreases the amplitude of targeted modes below their resistive-shell levels and shifts magnetic energy into m=1 modes with nearby resonant surfaces r_s (defined where $q(r_s)=m/n$), therefore also nearby in mode-number-space. As dominant modes are stabilized, they lose their dynamo character. As neighboring modes grow, they assume dynamo form. These newly-dominant fluctuations provide the RFP dynamo, whereas reversal is lost in the absence of feedback. The fluctuation-driven parallel electric fields of the new dynamo modes approach conducting-shell E_F profiles, sustaining reversal with low loop voltage.

4.2 Single-mode feedback

We performed nonlinear calculations for a R/a=2.5 RFP with S=6000 and θ=1.59. When the conducting shell at r=a is replaced with a resistive shell, loop voltage rises (Fig.1a) and reversal is lost on the order of a shell time (Fig.1b) Numerical tests were performed for two cases to test the feasibility of edge feedback on one internal tearing mode. $B_r(a)=0$ was imposed on the (m=1,n=-5) mode in one case and on the (1,-7) mode in another case. These are originally the dominant dynamo modes, typically resonating around r=.4a and r=.6a, respectively. Feedback on either dynamo mode sustains reversal and lowers loop voltage (Fig.1).

Improvement in plasma parameters of resistive-shell RFPs with feedback is due not simply to reductions in fluctuation levels, but to changes in E_F profiles. While feedback on (1,-5) reduces magnetic and velocity fluctuations in the targeted mode, fluctuations rise correspondingly in neighboring modes such as the (1,-7); similarly, (1,-7) feedback reduces (1,-7) fluctuations while (1,-5) fluctuations rise. While the overall fluctuation levels may increase or decrease with feedback, the relative phasing and spatial distribution of individual fluctuations can change such that volume-averaged E_F decreases, lowering V_L and sustaining reversal.

For example, without feedback (Fig.2a), E_F at the edge is insufficient to sustain reversal. Correspondingly, V_L quadruples in a shell time. With (1,-5) feedback, not only is reversal sustained, but loop voltage drops to within 30% of the conducting shell level as E_F drops throughout the plasma (Fig.2b). We find that feedback control of (1,-7) is not as effective in reducing V_L, pointing to a significant sensitivity to choice of target mode. Based on these single-mode feedback results, we attempt to more closely approach the conducting shell case

by applying feedback to several modes simultaneously.

4.3 Multi-mode feedback

4.3.1 Multi-mode feedback at small aspect-ratio

With either a conducting or resistive shell, tearing modes with m=1 and $|n| \approx 4$-8 dominate energy spectra in an RFP with aspect ratio R/a=2.5. The dominant m=1 modes tend to be separated by $\Delta n=2$, as the (0,2) mode is the largest axially symmetric fluctuation. Depending on the random amplitudes of initialized perturbations, we have found quasi-steady states where either (1,-5) and (1,-7) or (1,-4) and (1,-6) dominate the mode spectrum for several shell times. (Global plasma parameters such as mean field levels and profiles are generally independent of initalization.) These internally resonant helical fluctuations grow on the order of the resistive shell time in the absence of feedback. Loop voltage grows on a faster timescale in order to hold the plasma current constant. Most of the results presented here are from the initialization dominated by (1,-5) and (1,-7) fluctuations; results are comparable for the initialization dominated by (1,-4) and (1,-6) fluctuations.

Since the few m=1 modes with $|n|$ between 2R/a and 3R/a typically account for almost 90% of the fluctuation magnetic energy, we ran numerical tests of feedback on different combinations of these modes. Multi-mode feedback is applied to two and four modes in several combinations.

Feedback is applied to two modes simultaneously in four different cases: to (1,-5) and (1,-7); to (1,-4) and (1,-6); to (1,-5) and (1,-6). In a fourth test, feedback is applied to (1,-5) and (1,-7) until (1,-4) and (1,-6) become dominant, after which

time feedback is applied to (1,-4) and (1,-6). The (1,-5) tends to provide the bulk of the dynamo E_F in the absence of feedback. Stabilization of (1,-5) is common to the most effective feedback schemes: this channels energy into the (1,-4) and (1,-6) modes, which sustain dynamo with lower E_F. Feedback on (1,-4) or (1,-6), on the other hand, forces more energy into the original dynamo modes, (1,-5) and (1,-7), increasing fluctuations and V_L.

We also apply feedback to all four candidate dynamo modes simultaneously (m=1, |n|=4-7). In this case, energy does not flow into modes outside the candidate dynamo range, but peaks in (1,-5) again. Results are summarized in Fig. 3, which shows the approach of plasma loop voltage to the level in a conducting shell as feedback is applied to different modes. In all schemes which target (1,-5), growth rates approach zero for all modes as the feedback-stabilized RFP approaches steady state.

In the remainder of this section, we examine a limited set of runs in more detail to discern the mechanisms responsible for effective feedback. We focus on the simultaneous feedback of (1,-5) and (1,-7) modes in a resistive shell, and compare this case to the resistive shell without feedback (worst case) and to the conducting shell (best case), which effectively applies feedback to all fluctuations.

Fig.4 shows magnetic energy spectra for the three cases after evolution for one shell time. In the conducting-shell case, (1,-5) and (1,-7) are the dominant fluctuations. With a resistive shell, all modes grow approximately an order of magnitude in one shell time; (1,-5) remains dominant and (1,-6) has grown nearly as large as (1,-7) (Fig.4a) When feedback is applied to the two dominant modes simultaneously, the (1,-5) and (1,-7) amplitudes drop below conducting-shell levels. All other modes grow beyond conducting-shell levels, and the neighboring modes (1,-4) and (1,-6) become dominant, as seen in Fig 4b. Reversal is maintained past three shell times, when we choose to terminate the run.

(High velocity fluctuations in the case without feedback make the time step size too small to justify continuing our tests beyond this point.)

Modal $E_F(m,n)$ profiles change reproducibly when feedback is applied to dominant modes: these lose their dynamo character and the newly-dominant m=1 modes spontaneously alter to provide the dynamo instead. In the conducting-shell case, (1,-5) and (1,-7) drive dynamo with negative E_F in the reversal region. When feedback is applied to these modes they lose their dynamo character,contributing negligible E_F in the reversal region (Fig.5). The (1,-6) and (1,-4) were small and non-dynamo with a conducting shell. But in the feedback case, these neighboring modes adjust to provide negative E_F in the reversal region (Fig.6, curve b), taking on the dynamo role. (This process is representative of all feedback cases examined. For example, in the initialization which yields dominant (1,-4) and (1,-6) in steady state, feedback on these modes causes them to lose their dynamo character, while neighboring (1,-5) and (1,-7) grow to provide the dynamo.) As in single-mode feedback, reduced E_F keeps $E_{||}$ and V_L low for a given plasma current.

Since central E_F drops, the newly-dominant m=1 modes sustain the RFP more efficiently than the original, feedback-stabilized dynamo modes. The efficiency of the new dynamo modes can be quantified in terms of the ratio of dynamo-driving poloidal E_F near the RFP edge to current-suppressing toroidal E_F near the core. We define $\varepsilon = \langle E_{F\Theta} \rangle_{edge} / \langle E_{FZ} \rangle_{core}$, where $\langle \ \rangle_{edge}$ is a volume average from r_m to r=a and $\langle E_{FZ} \rangle_{core}$ is a volume average from r=0 to r_m, where the poloidal and toroidal fields have the same magnitude at r_m. For example, the (1,-6) dynamo mode in the feedback case yields $\varepsilon \equiv 21\%$. Without feedback the same dynamo mode has only $\varepsilon \equiv 11\%$, and significantly higher V_L is required to maintain the plasma current.

A scenario for the mechanism of feedback stabilization emerges from our

investigations. When $B_r(m,n)\,|_a = 0$ is applied to a dominant m=1 tearing mode resonant near axis, the mode's global B(r) and v(r) amplitudes decrease. As E_F drops on axis, central J can grow. This decreases the axial safety factor, shifting r_s inward for axially resonant modes. Deeper resonant surfaces result in relatively larger dynamo-driving regions of negative $(E_F)_\theta$ outside each $r_s(m,n)$. The net effect, as demonstrated above, is more RFP dynamo and less loop voltage.

Decomposition of $(E_F)_\theta \approx -\langle vxb\rangle_\theta = v_r b_z - v_z b_r$ for many feedback cases consistently shows that in resistive-shell RFPs the $v_r b_z$ term drives most of the negative mean E_θ, or dynamo, at the plasma edge in resistive-shell RFPs (Fig.7a). In conducting-shell RFPs, it is $v_z b_r$ which accounts for dynamo drive, since v_r is smaller throughout the reversal region than b_r. Similarly, examination of $(E_F)_z = v_\theta b_r - v_r b_\theta$ reveals that both terms contribute nearly equally to loop voltage (Fig.7b) in all cases. Experimental measurements of these terms are planned[25].

4.3.2 Multi-mode feedback at large aspect-ratio (R/a=6.0,

The number of dominant modes is about 2R/a. Hence, feedback can be more difficult at large aspect-ratio. The dominant fluctuations have higher n-number and are more closely spaced than in the small aspect-ratio cases considered above, since the safety factor on axis decreases as R/a increases, as seen in Fig.8. Tearing modes are more strongly coupled to each other; mode amplitudes and growth rates are also greater at large aspect ratio. In the absence of feedback, magnetic energy fluctuations grow and the loop voltage increases a factor of 4 in one shell time, as seen in Fig.9.

All internal m=1 modes in the range (1,-11) to (1,-18) contribute readily to the dynamo when R/a=6.0. If feedback is applied to any one of these candidate

dynamo modes, energy in that mode simply shifts into near neighbors. However, unlike the small-aspect ratio case, such a shift in the energy spectrum does not tend to lower the loop voltage. Feedback on (1,-13) alone, which tends to be slightly larger than the other dynamo modes, is insufficient to improve the efficiency of neighboring dynamo modes. Several m=1 modes must be stabilized simultaneously; significant loop voltage reduction is evident when the number of modes stabilized approaches the aspect ratio (Fig.9).

As an auxilliary method, we investigate feedback not just on m=1, but also on modes which play a role in m=1 coupling. Since m=1 modes couple to each other quasilinearly through m=0 modes as well as nonlinearly, m=0 feedback is added. If feedback of m=0 modes also reduced amplitudes of m=1 modes to which they couple, then feedback on only a few m=1 modes may suffice with simultaneous feedback on m=0. Combining m=1 feedback with (0,2) feedback is observed to reduce plasma V_L and feedback coil currents only to a moderate extent. Feedback on a wide range of candidate dynamo modes more closely approaches the conducting shell case.

Currents required by feedback coils (J_{FB}) remain relatively low, regardless of aspect ratio. At most, $(J_{FB})_{tot}/J_{plasma} \cong 8.5\%$ is required to decrease loop voltage by 60% when five dynamo modes are simultaneously stabilized. These results suggest that if space constraints are not severe, coils resonant with m=1, $2R/a < n < 3R/a$ should be wound for possible use in feedback stabilization. Addition of a (0,2) winding provides moderate feedback system flexibility.

4.4 Comparisons with experiment

4.4.1 Experimental observations

The HBTX1C RFP (R/a=3.0) experiment experienced higher fluctuation levels and truncated plasma discharge times when its conducting wall was replaced with a resistive shell.[2] Reversal loss was attributed to growing resistive shell modes. The resistive internal (1,-5) and ideal external (1,2) modes were observed to grow at similar rates at θ=1.6, contrary to predictions of linear theory[26], suggesting close nonlinear coupling between the modes. The internal mode resonates near the plasma axis, but the external mode is nonresonant. This suggested that feedback coils at the wall (r=1.1a) might more effectively suppress the free boundary (1,2) mode. It was hoped that suppression of (1,2) would couple to suppress (1,- 5) also, thereby sustaining the RFP. Feedback coils were wound outside a secondary shell at 1.1a with a 5.5 ms vertical field soak-in time. Reversal persisted up to two shell times with application of (1,2) feedback, but loop voltage and fluctuation levels remained high[10] .

4.4.2 MHD computations

Our low-aspect ratio calculations[7] model an RFP similar in size to HBTX . It should be noted that the high resistivity (low S) in our calculations, relative to experiment, yields smaller external kinks, such as the (1,2) mode.[15]

We modeled an idealization of the experimental feedback (which reduced B_r at r=1.1a with a finite time lag) with calculations that nulled B_r at r=a at all times. Our computations show that edge feedback on the (1,2) mode, resonant near the plasma edge, is less effective than edge feedback on a tearing mode resonant near axis. As seen in Fig.1, the resistive shell RFP loses reversal on the order of a shell time. Feedback on the external (1,2) mode makes edge E_F

sufficiently negative to sustain reversal (Fig.10), but fluctuation levels and V_L remain high, as in HBTX1C. While reversal lost with a resistive shell is restored with feedback on either the (1,2) or (1,-5) mode (section 4.2), only the latter also reduces V_L (Fig.11). This is because axial E_F remains high with (1,2) feedback (Fig.10), while (1,-5) feedback leads to reduced E_F throughout the plasma (Fig.2).

The similarity of experimental and numerical results suggests that even ideal feedback applied to external modes such as (1,2) is of limited use on an RFP. It is more effective to target the m=1 dynamo modes directly, instead of relying on coupling with externally resonant modes targeted for feedback. This is consistent with observations that axially resonant m=1 tearing modes drive RFP dynamics, through quasilinear modifications of mean field profiles and through nonlinear interactions with each other[8,9] . That edge feedback has a strong effect on dynamo modes even though they are resonant deep within the plasma need not be surprising in light of calculations[22] which found internal m=1 modes' dependence on boundary conditions to be highly nonlinear.

5. SUMMARY

The growth of tearing modes in resistive shell RFPs poses problems for potential RFP reactors. A simple feedback scheme has been developed to stabilize resistive shell fluctuations without suppressing the RFP dynamo. Investigation by nonlinear MHD computations on RFPs of large and small aspect ratio reveal that feedback on a small number (~R/a) of m=1 modes restores RFP reversal and lowers loop voltage. Edge feedback on axially resonant m=1 dynamo modes proves more effective than edge feedback on free-boundary or on edge-resonant modes which couple to m=1. A physical mechanism for feedback stabilization is

proposed. Feedback tests also reveal optimal $\langle \vec{v} \times \vec{b} \rangle$ profiles for dynamo efficiency and show that $v_r b_z$ provides the bulk of the resistive-shell RFP dynamo. Results agree with a limited experimental test of feedback on an external mode. Feedback stabilization of dominant internally resonant tearing modes is predicted to extend plasma lifetimes and reduce required loop voltage. This has yet to be tested experimentally.

This work was supported by the U.S. Department of Energy.

[1] TAMANO, T. BARD, W.D. CARLSTROM, T., et al., Plasma Physics and Controlled Nuclear Fusion Research 1986 (Proc. 11th Int. Conf. Kyoto, 1986), Vol.2, IAEA, Vienna (1987) 655
[2] ALPER, B., BEVIR, M.K., BODIN, H.A.B, et al., Plasma Phys. Controlled Fusion **31** (1989) 205
[3] GREENE, P., BARRICK, G., ROBERTSON, S., Phys. Fluids B **2** (1990) 3059
[4] MASAMUNE, S., US-Japan RFP workshop, University of Wisconsin, Madison, (March 1992)
[5] ROBINSON, D.C., Nucl.Fusion **24** (1984) 423
[6] HO, Y.L., PRAGER, S.C., SCHNACK, D.D., Phys.Rev.Lett.**62** (1989) 1504
[7] NILLES, E.J., PRAGER, S.C., HO, Y.L., Bull. Am. Phys. Soc. **34** (1989) 2147
[8] SCHNACK, D.D., CARAMANA, E.J., NEBEL, R., Phys. Fluids **28** (1985) 321
[9] HOLMES, J.A., CARRERAS, B.A., HENDER, T., et al.. in Controlled Fusion and Plasma Physics (Proc.16th Eur. Conf. Venice, 1989), Vol. 13B , Part II, European Physical Society (1989)
[11] BISHOP, C.M.,Culham Laboratory report CLM-P845 (1988)
[12] PLATT, C.L., ROBERTSON, S.H., IEEE Transactions on Plasma Science **19** (1991) 954
[13] SCHNACK, D.D., BARNES, D.C., MIKIC, Z. HARNED, D.S., CARAMANA,E.J., Jrnl. Comput.Phys. **70** (1987) 30
[14] HO, Y.L., PRAGER, S.C., Phys. Fluids **31** (1988) 1673
[15] GIMBLETT, C.G., SCHNACK, D.D., Simulation of the thin shell and secondary shell HBTX1C experiments, SAIC-91/1016:APPAT-140, Science Applications International Corporation, San Diego, CA (1991)
[16] SCHNACK, D.D., Magnetohydrodynamic theory of the Reversed-Field Pinch Dynamo, in Physics of Alternative Magnetic Confinement Schemes, S. Ortolani and E.Sindoni, Eds., SIF, Bologna, p.631 (1991)
[17] GOTTLEIB, D., ORSZAG, S.A., Numerical Analysis of Spectral Methods (SIAM, Philadelphia, PA 1977)
[18] HOLMES, J.A., CARRERAS, B.A., DIAMOND, P.H., LYNCH, V.E., Phys.Fluids **31** (1988) 1166
[19] TAYLOR, J.B., Rev. Mod. Phys. 58 (1986) 741
[20] LA HAYE, R.J., LEE, P.S.C., SCHAFFER, M.J., TAMANO, T., TAYLOR, P.L., Nucl.Fusion **28** (1988) 918
[21] ALMAGRI, A. et al., Workshop of Physics of Alternative Magnetic Confinement Schemes, Varenna, Italy, October 15-24, 1990
[22] HO, Y.L., PRAGER, S.C., Phys.Fluids B **3** (1991) 3099
[23] HO, Y.L., CRADDOCK, G.G., Phys. Fluids B **3** (1991) 721
[24] NEBEL, R.A., CARAMANA, E.J., SCHNACK, D.D., Phys.Fluids **B** 1 (1989) 1671
[25] DEN HARTOG, D.J., personal communication
[26] GIMBLETT, C.G., Proc.: Physics of Mirrors, Reversed Field Pinches and Compact Tori, Varenna, Vol.1 (1987) 241

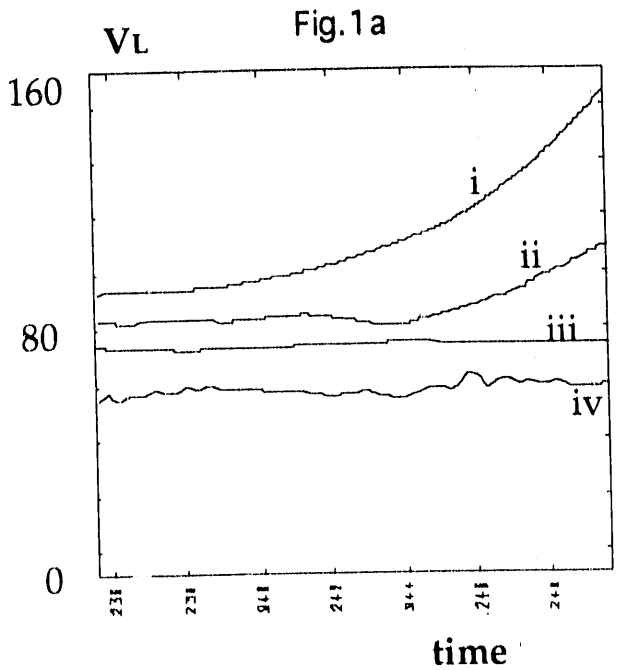

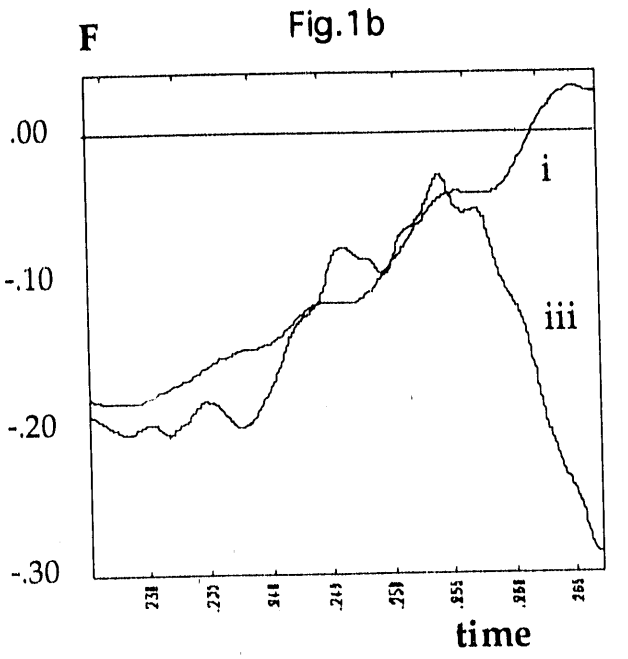

Fig.1: **a**) Loop voltage V_L versus time for three R/a=2.5 cases: **i**) resistive shell without feedback; **ii**) resistive shell with feedback on the (m=1, n=-7) mode; iii) resistive shell with feedback on (1,-5) mode; **iv**) close-fitting conducting shell. **b**) Reversal parameter $F=B_z(a)/\langle B_z\rangle$ versus time for **i**) resistive shell without feedback and **iii**) resistive shell with feedback on (1,-5) mode. F fluctuates about a mean value of -.20 in the steady state case with feedback.

Fig.2a

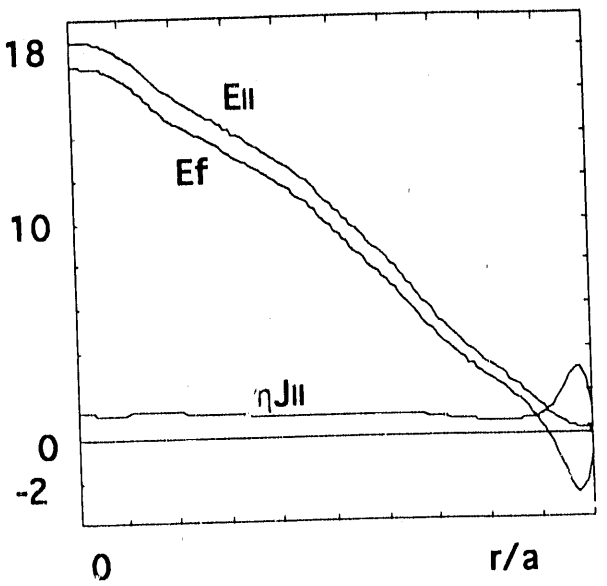

Fig.2b

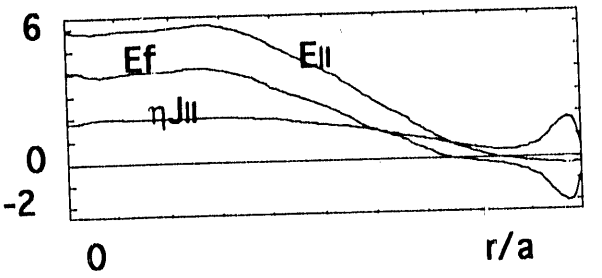

Fig.2 Radial profiles of total parallel electric field $E_{||}=E_F + \eta J_{||}$, E_F, and $\eta J_{||}$ where the parallel fluctuation-induced electric field $E_F = -S\langle vxb\rangle \cdot B/|B|$: **a)** without feedback and **b)** with (1,-5) feedback

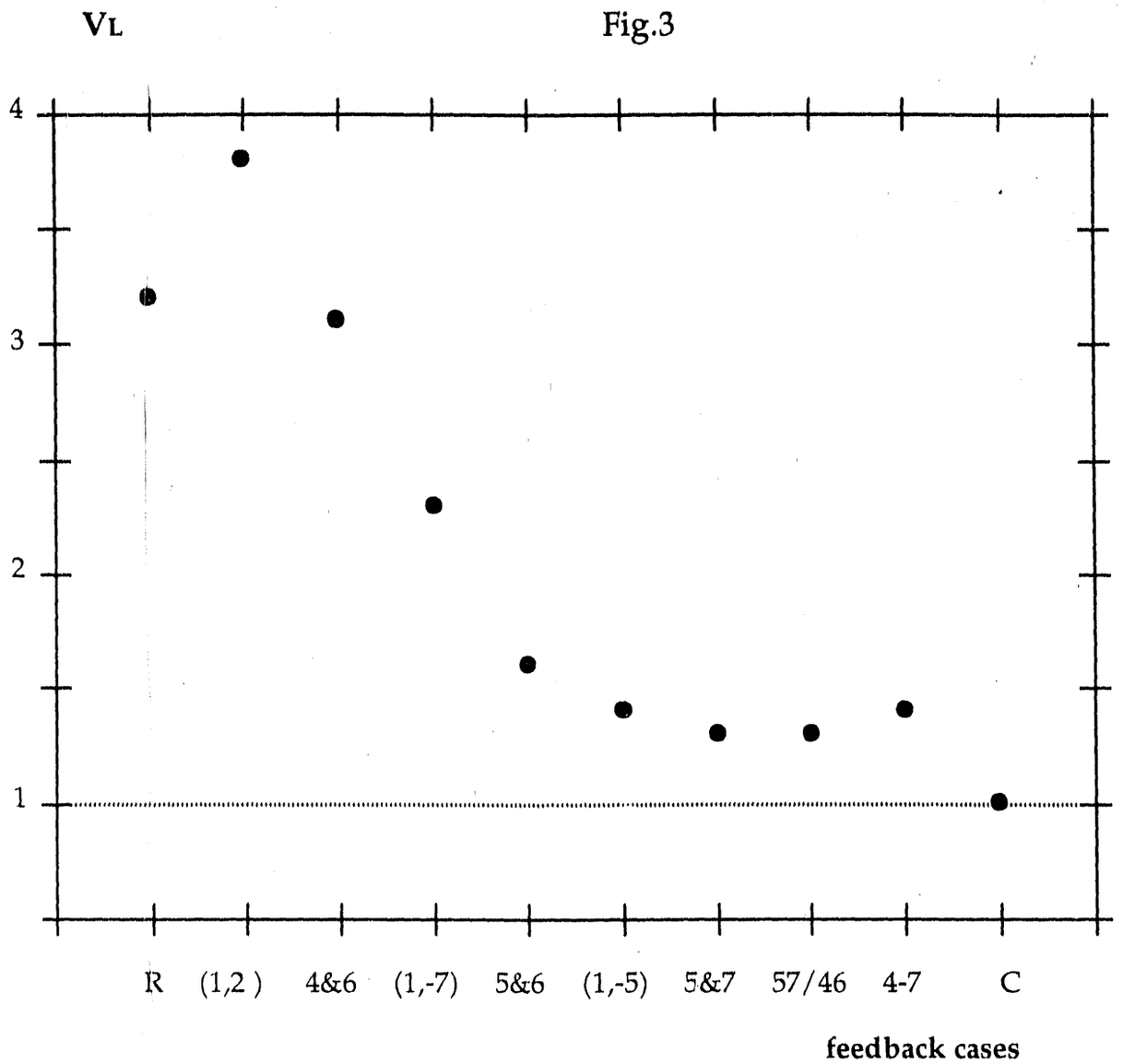

Fig.3: Loop voltage (normalized to conducting shell V_L) for different feedback cases (R/a=2.5): **R**: resistive shell without feedback; **(1,2)**: resistive shell with (1,2) feedback; **4&6**: resistive shell with (1,-4)&(1,-6) feedback; **(1,-7)**: resistive shell with (1,-7) feedback; **5&6**: resistive shell with (1,-5)&(1,-6) feedback; **(1,-5)**: resistive shell with (1,-5) feedback; **5&7**: resistive shell with (1,-5)&(1,-7) feedback; **57/46**: resistive shell with (1,-5)&(1,-7) then (1,-4)&(1,-6) feedback; **4-7**: resistive shell with (1,-4)&(1,-5)&(1,-6)&(1,-7) feedback; **C**: conducting shell

m=1 magnetic energy spectra

Fig.4a

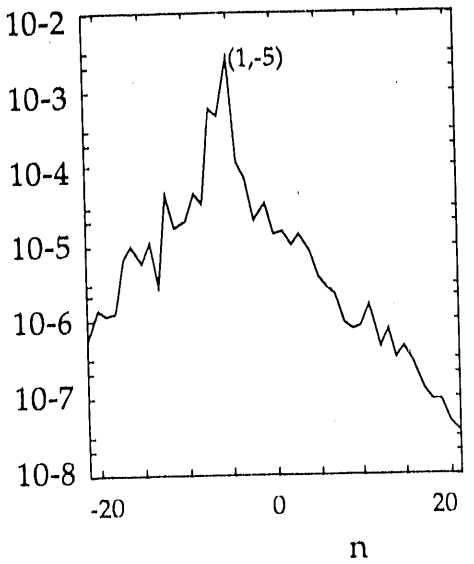

Fig.4b

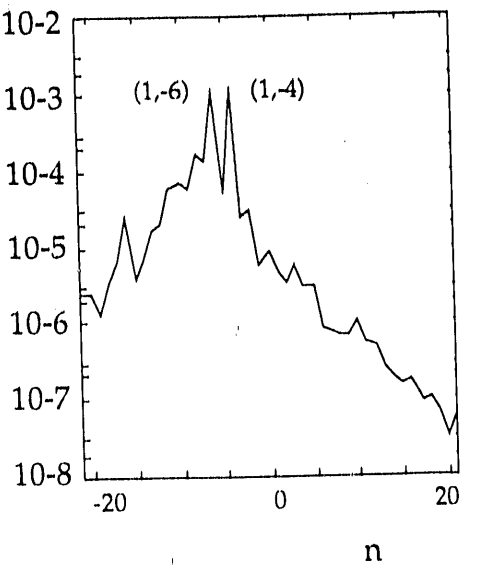

Fig.4c

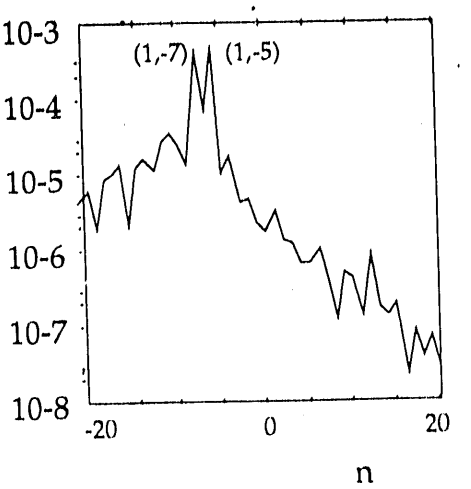

Fig.4: Spectra of m=1 magnetic energy fluctuations (volume-averaged) versus toroidal mode number n: **a**) resistive shell without feedback **b**) resistive shell with (1,-5) and (1,-7) feedback **c**) conducting shell

Fig.5

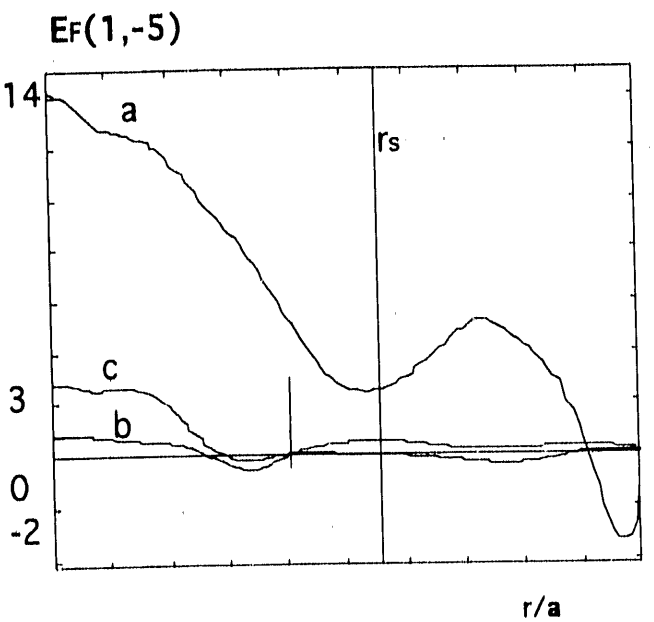

Fig.6

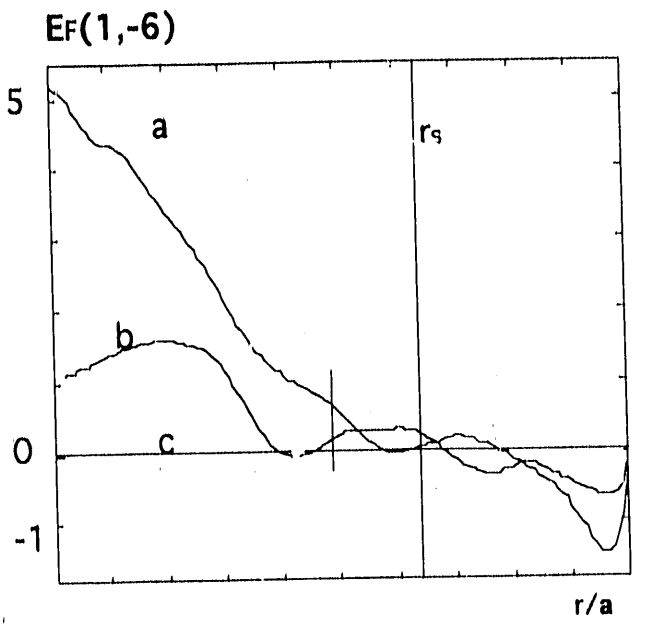

Figs.5: Profiles of modal (1,-5) fluctuation-induced electric field $E_F = \langle v \times b \rangle \cdot B / |B|$ for **a**) resistive shell without feedback; **b**) resistive shell with(1,-5)&(1,-7) feedback; **c**) conducting shell. Long vertical line is the resonant surface r_s without feedback; short vertical line is r_s for cases (b) and (c).

Fig.6: Profiles of modal (1,-6) fluctuation-induced electric field $E_F = \langle v \times b \rangle \cdot B / |B|$ for **a**) resistive shell without feedback; **b**) (1,-5) and (1,-7) feedback; **c**) conducting shell EF oscillates about zero at too low a level to distinguish, on this scale. Long vertical line is the resonant surface r_s without feedback; short vertical line is r_s for cases (b) and (c).

Fig.7.a

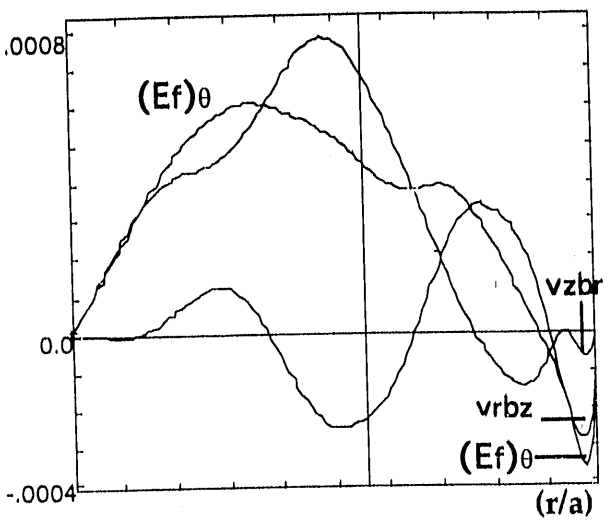

Fig.7.b

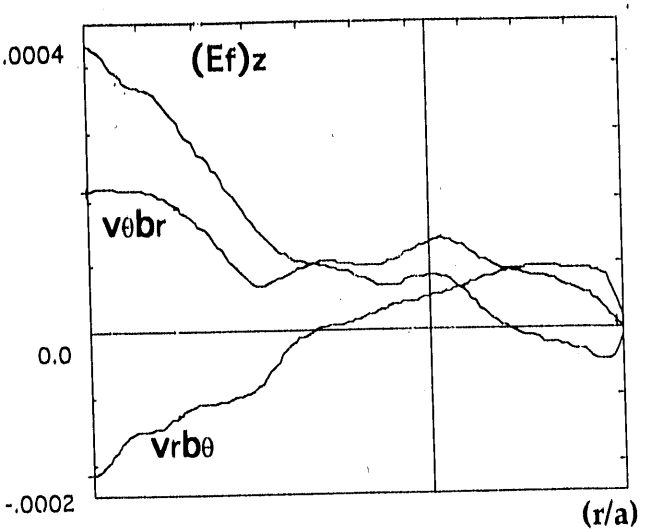

Fig.7: Resistive-shell profiles of: a) components of $(E_F)_\theta = v_r b_z - v_z b_r$ for (1,-5) b) components of $(E_F)_Z = v_\theta b_r - v_r b_\theta$ for (1,-6)

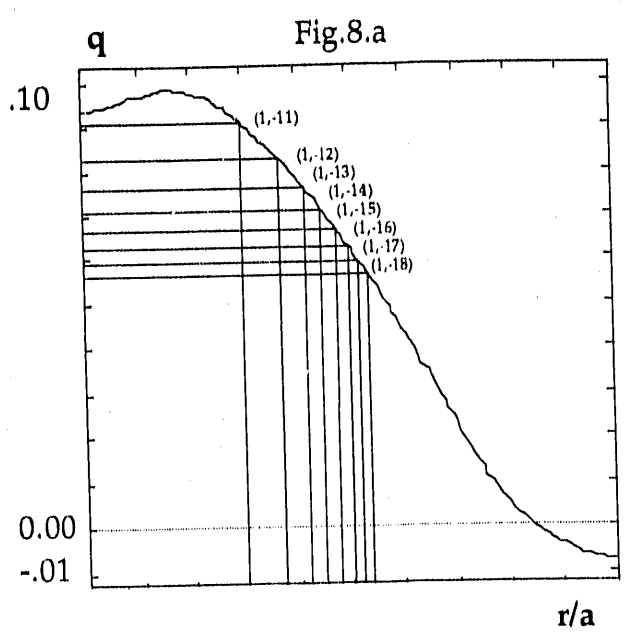

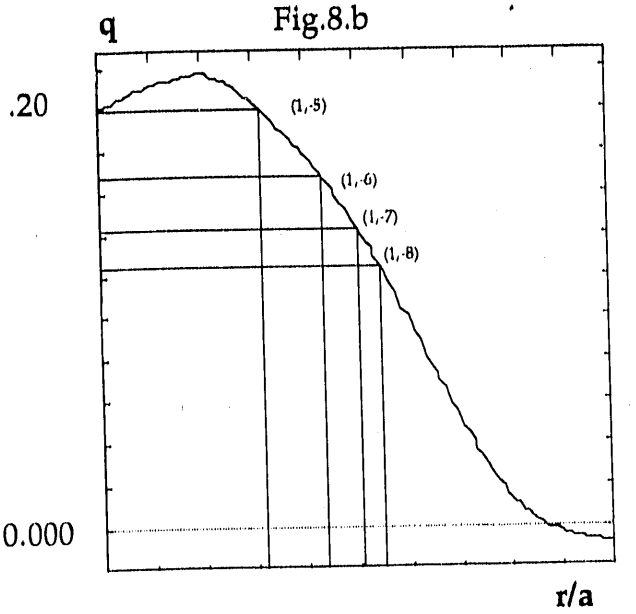

Fig.8: Safety factor profiles with resonant surfaces of dominant tearing modes for **a**) large aspect-ratio (R/a=6.0) steady state; **b**) small aspect-ratio (R/a=2.5) steady state

Fig.9

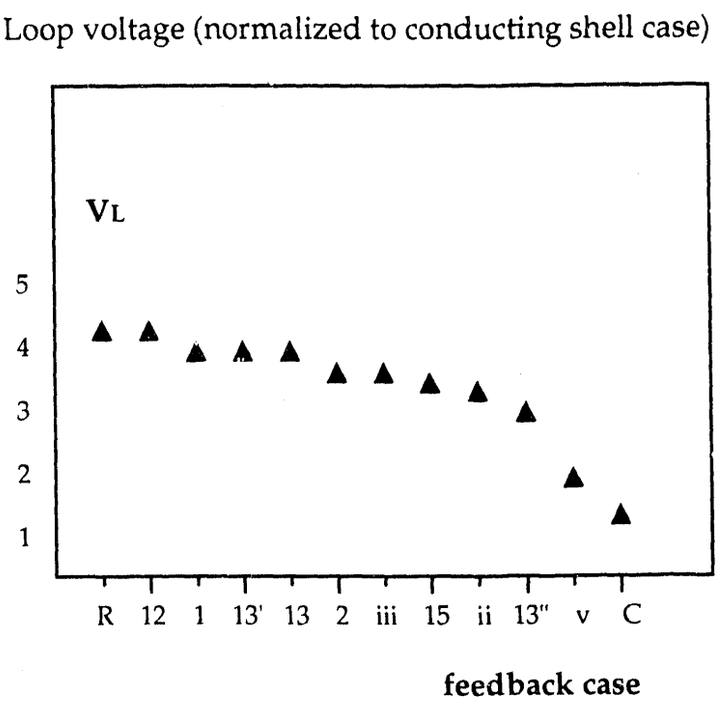

Fig.9: Loop voltage (normalized to conducting shell case for different R/a=6.0 feedback cases: **R**: resistive shell; **12**: resistive shell with (1,-12) feedback; **1**: resistive shell with (0,1) feedback; **13'**: resistive shell with (0,1)&(1,-13) feedback; **13**: resistive shell with (1,-13) feedback; **2**: resistive shell with (0,2) feedback; **iii**: resistive shell with (1,-11)&(1,-13)&(1,-15) feedback; **15**: resistive shell with (1,-15) feedback; **ii**: resistive shell with (1,-11)&(1,-15) feedback; **13"**: resistive shell with (1,-13)&(0,2) feedback; **v**: resistive shell with (1,-11)&(1,-12)&(1,-13)&(1,-14)& (1,-15) feedback

Fig.10 a

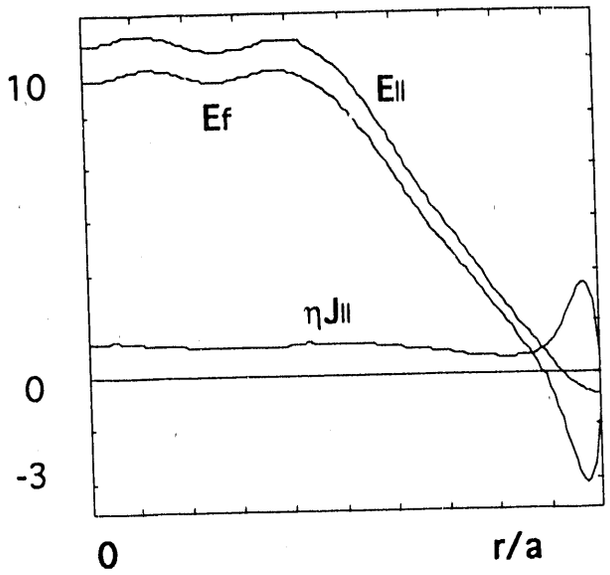

Fig.10 b

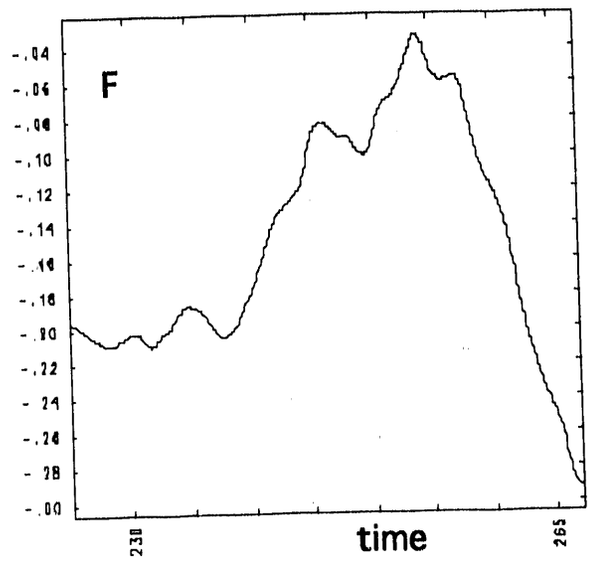

Fig.10. Resistive shell with feedback on (m=1,n=2) mode: **a**) Radial profiles of total parallel electric field $E_{||}=E_F + \eta J_{||}$, E_F, and $\eta J_{||}$ where parallel fluctuation-induced electric field $E_F = -S\langle vxb\rangle \cdot B/|B|$; **b**) Reversal parameter $F=B_z(a)/\langle B_z\rangle$ versus time

Fig.11

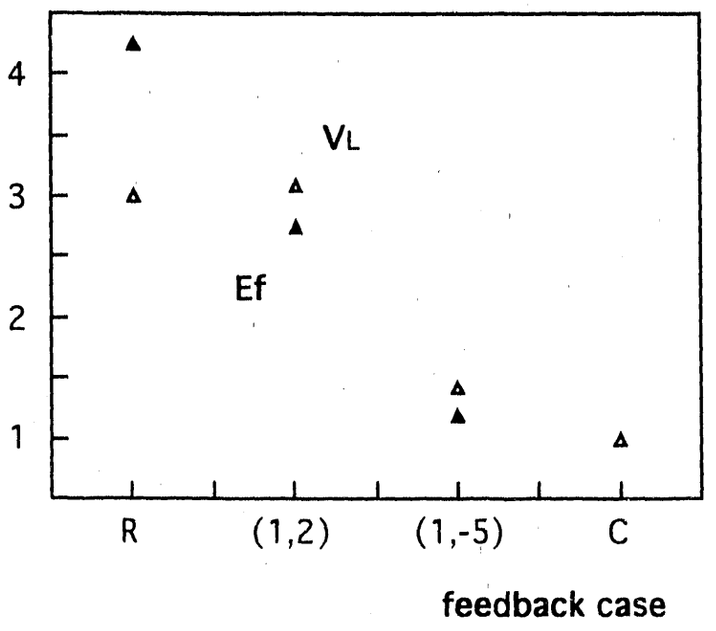

Fig.11: ▲ E_F=<vxb>versus feedback case: ▲ Loop voltage (normalized to V_L for consucting shell) versus feedback case. **R**: resistive shell without feedback; **(1,2)**: resistive shell with (1,2) feedback; **(1,-5)**: resistive shell with (1,-5) feedback; **C**: conducting shell

EXTERNAL DISTRIBUTION IN ADDITION TO UC-20

S.N. Rasband, Brigham Young University
J.B. Taylor, Institute for Fusion Studies, The University of Texas at Austin
M.A. Abdou, University of California, Los Angeles
R.W. Conn, University of California, Los Angeles
T. Dolan, INEL
R. Smith, University of Iowa
F.W. Perkins, PPPL
O. Ishihara, Texas Technical University
P.E. Vandenplas, Association Euratom-Etat Belge, Belgium
Centro Brasileiro de Pesquisas Firicas, Brazil
P. Sakanaka, Institute de Fisica-Unicamp, Brazil
Mme. Monique Bex, GANIL, France
J. Radet, CEN/CADARACHE, France
University of Ioannina , Greece
S. Ortolani, Istituto Gas Ionizzati, EURATON-ENEA-CNR Association, Italy
R. Andreani, Associazione EURATOM-ENEA sulla Fusione, Italy
Y. Kondoh, Gunma University, Kiryu, Gunma, Japan
H. Toyama, University of Tokyo, Japan
FOM-Instituut voor Plasmafysica "Rijnhuizen", The Netherlands
Z. Ning, Academia Sinica, People's Republic of China
P. Yang, Shandong University, People's Republic of China
S. Zhu, University of Science & Technology of China, People's Republic of China
I.N. Bogatu, Institute of Atomic Physics, Romania
M.J. Alport, University of Natal, Durban, South Africa
R. Storer, The Flinders University of South Australia, South Australia
B. Lehnert, Royal Institute of Technology, Sweden
Librarian, CRPP, Ecole Polytechnique Federale de Lausanne, Switzerland
B. Alper, Culham Laboratory, UK
A. Newton, Culham Laboratory, UK

6 for Chicago Operations Office
4 for individuals in Washington Offices

INTERNAL DISTRIBUTION IN ADDITION TO UC-20
80 for local group and file

END

DATE FILMED

7/7/92